ISSN 1330-3651 (Print), ISSN 1848-6339 (Online)
Received: 18 February 2025; Accepted: 1 June 2026

https://doi.org/10.17559/TV-20250218002388
Original scientific paper

High-Precision Vibration Signal Acquisition and Processing Technology for Industrial Equipment Monitoring

Guofu WEI*, Guanlin WANG

Abstract: In modern industry, vibration, as a common physical phenomenon during equipment operation, contains rich information about the internal state of the equipment. By collecting, processing, and analyzing vibration data, abnormal situations of the equipment can be detected promptly to prevent potential failures. However, the vibration signals of industrial equipment often exhibit nonlinear and non-stationary characteristics. Traditional signal processing methods are difficult to accurately capture these complex features, resulting in insufficient accuracy and low computational efficiency. This study uses a complementary set empirical mode decomposition of vibration signals and introduces sample entropy to make an improvement. At the same time, a high-precision vibration signal acquisition and processing technology for industrial equipment monitoring is designed by using discrete wavelet transform to process vibration characteristics. The results showed that compared with other methods, the proposed algorithm has improved accuracy by 8.06% and 10.49%, reduced rejection rate and false acceptance rate by 3.72% and 5.83%, and significantly reduced computation time, proving its high accuracy and computational efficiency. The coefficient of determination of the proposed algorithm was 0.987, which was higher than that of the comparison method, proving its high-fitting performance in practical applications. This algorithm effectively improves the accuracy and efficiency of industrial equipment vibration signal monitoring, providing strong support for early fault diagnosis and stable operation of industrial equipment. This is of great significance for promoting the development of industrial intelligent manufacturing.

Keywords: collection; empirical mode decomposition; handle; industrial equipment; vibration signal; wavelet transform

1 INTRODUCTION

Mechanical automation has become the development trend of factories today, and the precision industrial production process requires increasingly high requirements for motors and related mechanical equipment. Managers not only need to ensure its efficiency and reliability but also demand its consistent operation [1]. During the operation of mechanical equipment, if components fall off, the equipment ages, or the fixation is not firm, it will transform into abnormal vibration of the equipment, forming a safety hazard [2]. To constantly supervise machinery, it is necessary to rely on professional technicians to conduct real-time inspections of equipment on site, or to spend a lot of time and cost training production personnel [3]. Moreover, there are many minor accidents during the production process that are difficult to detect, and even experienced technicians may not be able to detect them promptly. The advancement of artificial intelligence technology has filled the gap in this field with the emergence of Vibration Signal Acquisition and Processing (VSAP) technology for industrial equipment. This technology can detect abnormal situations of mechanical equipment promptly and provide corresponding alarm prompts by monitoring the vibration of the equipment in real-time. This can avoid production accidents caused by equipment failures. Moreover, it is possible to predict potential equipment problems in advance and take timely measures for maintenance or replacement, thereby reducing equipment maintenance costs and downtime, and improving production efficiency [4]. However, the existing technology for collecting and processing vibration signals of industrial equipment still faces many challenges. Fourier transform, local mean decomposition, and other methods suffer from insufficient accuracy and efficiency in processing nonlinear and non-stationary signals. Although empirical mode decomposition algorithm can improve accuracy by adding white noise to alleviate mode aliasing, it has a large computational complexity and significant residual noise interference [5]. Given this, this study first uses Complete Ensemble Empirical Mode Decomposition (CEEMD) to collect Industrial Equipment Vibration Signals (IEVSs). In addition, by optimizing the CEEMD algorithm using Sample Entropy (SE), a CEEMD-SE algorithm is designed to obtain vibration characteristics of industrial equipment. Then, using Wavelet Transform (WT) to process the vibration characteristics, a high-precision VSAP technology for industrial equipment monitoring is designed to improve the monitoring accuracy and efficiency of IEVS.

2 RELATED WORKS

In recent years, with the popularization of Industry 4.0 and intelligent manufacturing concepts, high-precision VSAP technology has played a crucial role in ensuring health monitoring and predictive maintenance of industrial equipment. Many scholars have achieved significant research results in this field. Iqbal et al. designed a vibration acoustic signal CNC machine tool-bearing fault detection method built on Convolutional Neural Network (CNN) to detect second-generation bearing faults in CNC machine tools. It converted the raw signals of vibration and sound signals into time-frequency analysis through short-time Fourier Transform (FT) and used CNN for diagnosing faults. This method had high classification accuracy for vibration and acoustic signals in fault detection [6]. Chu et al. designed a machining state recognition model grounded on approximate entropy Support Vector Machine (SVM) and short-time FT-CNN to identify the vibration conditions generated during the machining process of CNC milling machines. It utilized the characteristics of entropy and short-time FT to characterize the extracted processing signals as training models and used *k*-Fold Cross Validations (FCV) criteria to represent the recognition results. This method had a high recognition rate and training efficiency [7]. Hajji et al. constructed an adaptive feature learning algorithm built on deep CNN to deal with traditional vibration signal feature extraction methods being difficult to adapt to complex working

conditions. By introducing transfer learning strategies, this algorithm could demonstrate higher generalization ability and accuracy in different types of mechanical fault diagnosis, especially suitable for early fault detection [8]. Hosseinpour Zarnaq et al. designed a fault diagnosis method for tractor auxiliary transmissions based on vibration analysis and Random Forest (RF) classification to enhance the precision of fault diagnosis. It adopted discrete WT to process the collected vibration signals and used RF and multi-layer perceptron neural networks to classify the data, with high detection accuracy [9]. Mohammed et al. designed an industrial equipment fault prediction approach built on the Internet of Things (IoT) and Machine Learning (ML) to identify potential issues with industrial equipment. It integrated industrial IoT, message queue telemetry transmission, and ML algorithms to collect real-time data based on vibration signals, current, and temperature sensors. Multiple ML algorithms were used to predict motor faults with high accuracy [10].

Aljemely et al. designed a combined fault diagnosis method combining LSTM and a large interval nearest neighbor algorithm for rolling bearing fault diagnosis. It utilized orthogonal mass initialization technology to memorize the vibration signals of faults during parameter updates. This method surpassed other models in diagnostic efficiency, stability, and reliability [11]. Chen et al. designed a dual-scale first-layer kernel CNN fault prediction model for railway switch machines based on vibration models. It utilized a dual-scale structure combined with two time scales to suppress noise and extract vibration signals through the first layer kernel. This model had high robustness and accuracy [12]. Cai designed a tool state recognition method based on SSA-optimized variational mode decomposition to address the difficulty of extracting machine tool state feature information. It utilized an optimized algorithm to decompose the tool vibration signal and extract the kurtosis index and margin factor of the intrinsic mode function to form a feature vector. SVM was utilized to identify the tool state model. This method had better recognition accuracy than other algorithms [13]. Gu et al. designed a method based on the variational mode decomposition method for parameter optimization and permutation entropy to effectively extract the features of bearing vibration signals for fault diagnosis. It used a genetic algorithm to optimize parameter combinations with SE minimization as the indicator, and constructed evaluation indicators using mean square error and correlation coefficient to optimize the decomposition effect of variational mode decomposition. This method had high diagnostic accuracy [14]. Al Haddad et al. designed a fault state prediction method built on a gradient propulsion ML model for the health monitoring of permanent magnet synchronous motors. It integrated vibration signals and current data, utilized feature selection information to identify key attributes for fault assessment, and used the selected features to distinguish fault states, with high reliability [15].

In summary, although existing research has made some progress in VSAP, it still faces problems such as high computational resource consumption and insufficient algorithm generalization ability in practical applications. To address these challenges, a VSAP technology based on CEEMD-SE-WT has been proposed. This method first uses EMD to decompose complex vibration signals into several intrinsic mode functions and then uses WT to perform multi-scale analysis on each intrinsic mode function to extract more refined fault features. This study aims to improve the accuracy and real-time performance of fault diagnosis, providing strong guarantees for the secure operation of industrial equipment.

3 EMD-WT VSAP TECHNOLOGY FOR INDUSTRIAL EQUIPMENT MONITORING

This section mainly elaborates on the implementation of industrial equipment VSAP technology based on EMD-WT. The first subsection is the implementation of the EMD-based IEVS acquisition algorithm, and the second subsection is the function design of the WT-based IEVS processing technology.

3.1 IEVS Acquisition Algorithm Based on EMD

In modern industry, the analysis and processing of equipment vibration signals are particularly important. Many mechanical failures are accompanied by abnormal vibrations. Vibration signals are signals generated during the operation of mechanical equipment, which contain information including the operating conditions and faults of the equipment. Therefore, by conducting an in-depth analysis of the characteristics of vibration signals, it is possible to effectively diagnose equipment faults and evaluate performance. Firstly, it is necessary to collect industrial equipment signals. By collecting and analyzing vibration signals, the operating status of mechanical equipment can be understood. The traditional industrial equipment VSAP technology mainly includes FT, local mean decomposition, SVM, etc. However, these methods suffer from low accuracy and efficiency in processing vibration signals. EMD algorithm is a time-frequency signal processing method that decomposes signals built on the time scale features of the data itself, without the requirement to pre-set any basis functions. It has benefits in processing non-stationary and non-linear data, fitting in analyzing signal sequences, and has a high SNR [16]. Therefore, this study adopts CEEMD developed on the basis of the EMD algorithm for IEVS acquisition and introduces SE to improve it, designing a vibration signal acquisition algorithm based on CEEMD-SE. The framework of the CEEMD-SE algorithm is shown in Fig. 1.

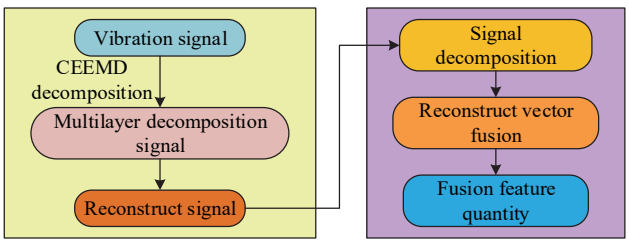

Figure 1 CEEMD-SE algorithm framework

Fig. 1 shows the decomposition method of complex signals. It is decomposed into several physically meaningful intrinsic mode functions. Firstly, a Gaussian White Noise (GWN) is added and the input vibration signal

is added and subtracted to obtain a new signal, as expressed in Eq. (1).

$$y_n(t) = y(t) + \varepsilon_0 \delta_n(t) \tag{1}$$

In Eq. (1), $y_n(t)$ means the obtained new signal sequence. $y(t)$ is the input vibration signal. ε_0 denotes the noise coefficient added to the input sequence by CEEMD at a certain stage. $\delta_n(t)$ is the GWN during the n-th processing. Then, the obtained new signal is subjected to EMD, and its mean is taken as the first intrinsic mode component of CEEMD, while obtaining the residual sequence. The calculation method is shown in Eq. (2).

$$\begin{cases} c_1(t) = \dfrac{1}{N}\sum_{N}^{n=1} c_1^n(t) \\ r_1(t) = y(t) - c_1(t) \end{cases} \tag{2}$$

In Eq. (2), $c_1(t)$ is the first eigenmode component. N is the total amount of times that GWN is added. $r_1(t)$ is the first residual sequence obtained. Next, the residual sequence is added with GWN to construct N new sequences, and these N sequences are further subjected to EMD, averaged, and subtracted to obtain the residuals of the m-stage, as shown in Eq. (3).

$$r_m(t) = r_{m-1}(t) - c_m(t) \tag{3}$$

In Eq. (3), $r_m(t)$ is the residual of stage m, representing the intrinsic modal components of stage m. Subsequently, the EMD operation is repeated to obtain the vibration signal after CEEMD, as expressed in Eq. (4).

$$y'(t) = R(t) + \sum_{M}^{m=1} c_m(t) \tag{4}$$

In Eq. (4), $y'(t)$ means the final output signal sequence, and $R(t)$ is the final residual sequence. The implementation path of CEEMD algorithm is shown in Fig. 2.

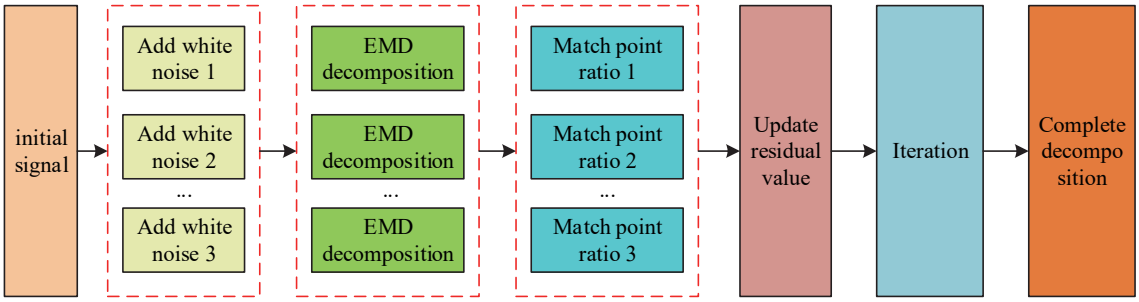

Figure 2 Implementation path of CEEMD algorithm

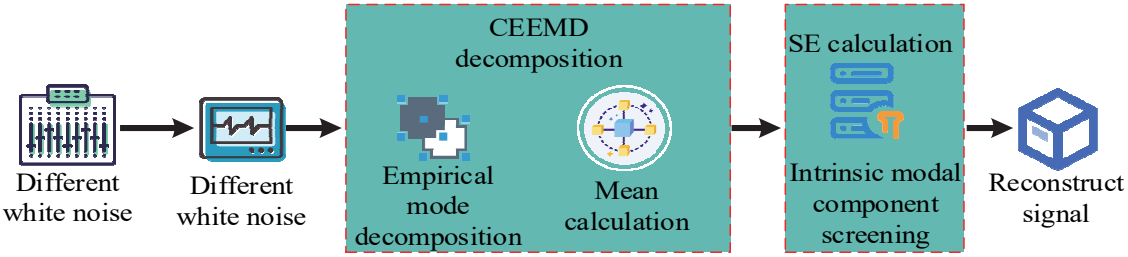

Figure 3 Flow of vibration signal acquisition algorithm based on CEEMD-SE algorithm

In Fig. 2, the CEEMD algorithm requires multiple EMD processes during signal decomposition. Each time, it is required to conduct EMD on the signal, and then combine the various eigenmode functions obtained from the decomposition.

This process requires repeated iterations, resulting in a high time complexity of the algorithm. Therefore, this study introduces SE to optimize it. SE is an indicator utilized to measure the complexity of time series. Compared with other complexity indicators, it has the advantages of simple calculation and insensitivity to data length, making it more suitable for analyzing shorter time series. The smaller the SE value, the stronger the regularity and lower the complexity of the time series, while a larger SE value indicates stronger randomness and complexity of the time series. After CEEMD, SE can be calculated separately for each eigenmode component to analyze the complexity of each scale and shorten the computation time [17]. The formula of SE is given by Eq. (5).

$$S(d, i, L) = -\log\left(\frac{C(d, i)}{C(d-1, i)}\right) \tag{5}$$

In Eq. (5), d is the embedding dimension, i is the tolerance, L means the length of the time series. $C(d, i)$ denotes the proportion of matching points. The implementation path of the proposed vibration signal acquisition algorithm based on CEEMD-SE algorithm is shown in Fig. 3.

In Fig. 3, a series of intrinsic modal components and their corresponding SEs can ultimately be obtained. By analyzing the time and frequency domain features of these components, as well as the SE of each component, the composition of the time series can be understood, thereby completing the acquisition of vibration signals.

3.2 IEVS Processing Technology Based on Improved WT

The CEEMD-SE algorithm achieves high-precision acquisition of vibration signals through adaptive decomposition and SE optimization. However, in actual industrial environments, signals are often accompanied by complex noise interference, and further processing is needed to improve the reliability of feature extraction. Although traditional processing methods such as FT have made significant contributions in frequency domain analysis, they have limitations in analyzing non-stationary signals. This is because these methods cannot simultaneously provide local information in both domains [18]. The emergence of WT provides an effective way to solve this problem. WT is a time-frequency analysis method that can provide high-resolution information in both domains simultaneously. This makes it very suitable for analyzing non-stationary signals such as mechanical equipment vibration. Through WT, vibration signals can be decomposed into wavelet coefficients of different scales and time positions. These coefficients can reflect the frequency components of the signal at various times, thereby revealing various features hidden in the vibration signal [19]. Therefore, in this study, WT is taken to further process the extracted signals. The implementation path of WT is shown in Fig. 4.

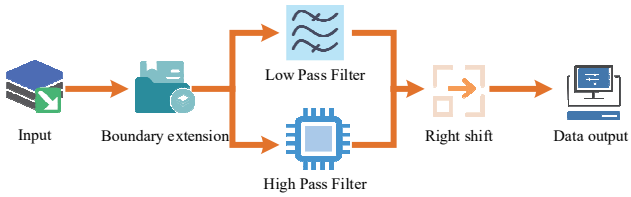

Figure 4 WT algorithm process

In Fig. 4, WT is divided into continuous WT and discrete T. Among them, continuous WT is a mathematical tool utilized to analyze various kinds of functions, which is fit in handling data with continuous changes and no obvious discrete characteristics. Discrete WT can provide time-frequency features of data and has the ability to decompose at multiple scales, making it extensively utilized in signal denoising, feature extraction, compression, and other fields [20]. Therefore, this study adopts discrete WT for vibration signal processing. Firstly, the autocorrelation sequence of noise is defined as shown in Eq. (6).

$$\rho(k)=\begin{cases}1, k=0\\0, k\neq 0\end{cases} \tag{6}$$

In Eq. (6), $\rho(k)$ is the autocorrelation sequence of noise, and k is the k-th sequence. Then, the collected vibration signal is input, and its autocorrelation sequence is shown in Eq. (7).

$$|\rho_i|\le\frac{\xi}{\sqrt{K}}, i\ge 1 \tag{7}$$

In Eq. (7), ρ_i is the data sequence of the collected vibration signal. K is the discrete data sequence's length. ξ means the threshold for determining whether a discrete data sequence is a white noise sequence, with a value of 1.95. If the autocorrelation sequence satisfies the condition in Eq. (7), then the noise sequence belongs to a white noise sequence [21]. Next, the vibration signal sequence is input, and the discrete WT calculation method is given by Eq. (8).

In Eq. (8), $W(a, b)$ is the transformation coefficient, Ψ^* is the complex conjugate of the wavelet function. a and b are the scale and translation parameters. By adjusting the translation parameter, the position of the wavelet function on the time axis can be changed, thereby matching it with the signal at different time positions [22].

$$W(a,\ b)=\int_{-\infty}^{\infty}y'(t)\Psi^*\left(\frac{t-b}{a}\right)\mathrm{d}t \tag{8}$$

Next, the inner-product of the vibration signal and the wavelet function is calculated to obtain the WT coefficient of the signal, as shown in Eq. (9).

$$\left\langle y'(t),\ \Psi(t)\right\rangle=\int_{-\infty}^{\infty}y'(t)\Psi^*(t)\mathrm{d}t \tag{9}$$

In Eq. (9), $\Psi(t)$ is a wavelet function. The discrete WT is displayed in Fig. 5.

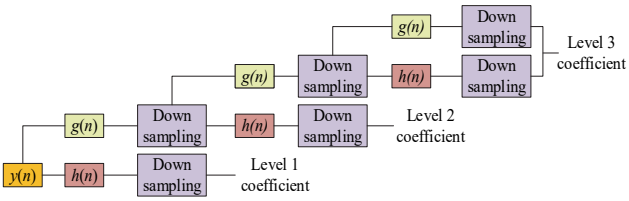

Figure 5 Discrete wavelet transform

The next step is to replace the wavelet function with Morlet, as expressed in Eq. (10).

$$\Psi(t)=\pi^{-\frac{1}{4}}e^{r\omega_0 t}e^{-\frac{t^2}{2}} \tag{10}$$

In Eq. (10), ω_0 is the frequency parameter, r is the imaginary unit, and π is the pi. WT needs to extract time-frequency features by calculating the inner product of the signal and wavelet function, while the complex domain inner product operation requires complex conjugation of the wavelet function to maintain amplitude and phase information. Therefore, it is necessary to perform complex conjugate calculation on the Morlet wavelet function to obtain the update of the Morlet wavelet function. The calculation method is shown in Eq. (11).

$$\Psi'_{a,\ b}(t)=\pi^{-\frac{1}{4}}e^{i\omega_0(t-b)}e^{-\frac{(t-b)^2}{2a^2}} \tag{11}$$

In Eq. (11), $\Psi'_{a,\ b}(t)$ is the Morlet under the scale parameter and translation parameter. The next step is to obtain the transformation formula of Morlet wavelet, as shown in Eq. (12).

$$W(a,b)=\int_{-\infty}^{\infty}x(t)\pi^{-\frac{1}{4}}e^{i\omega_0(t-b)}e^{-\frac{(t-b)^2}{2a^2}}\,dt \tag{12}$$

In Eq. (12), $W(a, b)$ is the transform coefficient of the Morlet wavelet. At this point, the processing of IEVS has been completed. The process flow of IEVS processing technology based on improved WT is shown in Fig. 6.

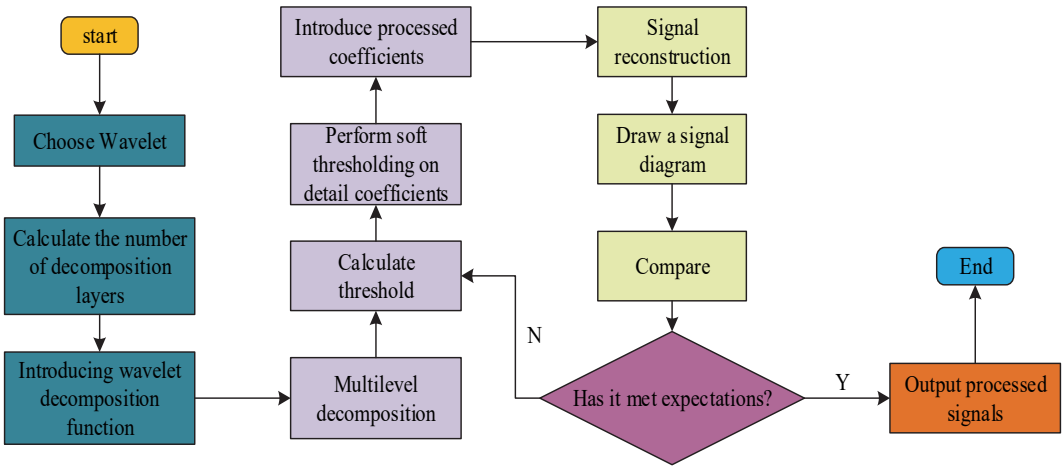

Figure 6 Feature recognition of IEVS based on improved WT

4 INDUSTRIAL EQUIPMENT VSAP TECHNOLOGY BASED ON CEEMD-SE-WT

This section mainly elaborates on the experimental results of the high-precision VSAP technology proposed for industrial equipment monitoring. Subsection 1 is the performance analysis of industrial equipment VSAP technology based on CEEMD-SE-WT. Subsection 2 is the practical application effect analysis of industrial equipment VSAP technology based on CEEMD-SE-WT.

4.1 Performance Analysis of Industrial Equipment VSAP Technology Based on CEEMD-SE-WT

To verify the effectiveness of the high-precision VSAP technology designed for industrial equipment monitoring, this study used an Intel Core i7-10700 central processor, CUDA Toolkit 12.3 graphics processor, RTX 4070 Ti graphics card, 64 GB of RAM, and Windows 11 operating system. MATLAB 2022b programming language was also utilized for simulation experiments. The experimental environment was set up in a certain ultra-low frequency vibration monitoring experimental center. The experimental process included three modules: data acquisition, signal preprocessing, and feature extraction. The data acquisition module converted the collected analog signals into digital signals through the YD980 eddy current sensor and transmitted them to the computer through the USB interface. In the signal preprocessing stage, CEEMD-SE was used to decompose and extract features from the collected vibration signals. Finally, WT was used to further process and analyze the extracted feature signals, thereby completing the collection and processing of equipment vibration signals. The number of iterations was 1000. Firstly, the CWRU dataset was used to train the algorithm and calculate the loss and accuracy of the designed algorithm. The CWRU dataset was one of the widely used standard datasets in the field of mechanical fault diagnosis. It recorded normal operating conditions as well as different types of bearing fault states, including bearing inner and outer rings and rolling element damage. Each fault condition also distinguished different fault sizes and load conditions, providing researchers with rich fault signal data and enabling them to develop and validate various data analysis, feature extraction, and ML algorithms. Fig. 7 shows the comparison results with traditional EDM and the method in reference [20].

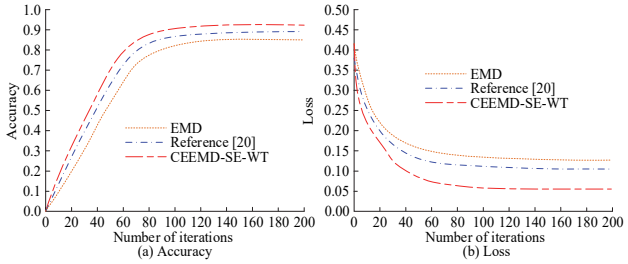

Figure 7 Loss and accuracy of various models

In Fig. 7a, the accuracy gradually increases and tends to plateau. Among them, when the accuracy curve of traditional EMD tends to stabilize, the accuracy is 0.85. When the accuracy curve of the method in reference [20] tends to stabilize, the accuracy is 0.90. The accuracy curve of the CEEMD-SE-WT algorithm reaches a stable accuracy of 0.93. In Fig. 7b, the loss curves of the three algorithms show a gradually decreasing trend and tend to stabilize. When the loss curves of the three algorithms tend to stabilize, the loss values are 0.12, 0.10, and 0.0.6. The accuracy of the designed algorithm is higher than others, while the algorithm loss is lower, which proves the high accuracy of the CEEMD-SE-WT algorithm and its superiority in IEVS processing. In the CWRU bearing dataset, the Precision, Rejection rate, False Acceptance Rate (FAR), and Average Computation Time (ACT) of different algorithms are calculated through two 5 × 10 FCVs, and the standard deviation of accuracy is calculated. Comparisons are made with the methods in EMD, reference [19], and reference [20], as shown in Tab. 1.

In Tab. 1, during the first FCV, the precision of the CEEMD-SE-WT algorithm was 92.84%, the rejection rate was 4.62%, the FAR was 8.45%, and the ACT was 14.22s. The second FCV was 90.11%, 5.33%, 10.73%, and 12.43 seconds. During the first FCV, compared to traditional EMD and methods in references [19] and [20], the CEEMD-SE-WT algorithm improved precision by 8.06%, 3.47%, and 4.15%, decreased rejection rates by 3.72%, 5.11%, and 4.25%, and reduced FAR by 5.83%, 4.83%, and 2.82%. During the second FCV, the CEEMD-SE-WT algorithm improved precision by 10.49%, 6.53%, and 3.85%, decreased rejection rates by 3.36%, 3.99%, and 4.24%, and reduced FAR by 5.19%, 3.44%, and 2.51%.

Table 1 The precision, rejection rate, and FAR of different models

Number of experiments	Model	Precision / %	Rejection rate / %	FAR / %	Computation time / s	Precision standard deviation / %
First time	EMD	84.78	8.34	14.28	38.73	0.84
	Reference [19]	89.37	9.73	13.68	29.35	0.56
	Reference [20]	88.69	8.87	11.27	21.26	0.61
	EMD-WT	92.84	4.62	8.45	14.22	0.21
Second time	EMD	79.62	8.69	15.92	39.56	0.79
	Reference [19]	83.58	9.32	14.17	27.78	0.63
	Reference [20]	86.26	9.57	13.24	24.65	0.68
	EMD-WT	90.11	5.33	10.73	12.43	0.19

Meanwhile, in both cross validations, the computation time of the CEEMD-SE-WT algorithm was lower than the other methods, and the precision standard deviations of the CEEMD-SE-WT algorithm were 0.21 and 0.19, respectively, lower than the other methods. The above results indicated that the CEEMD-SE-WT algorithm had high precision and low rejection rates, as well as low time complexity and high stability, demonstrating its superior performance in IEVS processing. To further validate the performance of the algorithm, this study calculated the Precision, Recall, and Area Under the Curve (AUC) of the CEEMD-SE-WT algorithm in two separate experiments. The comparison with traditional EMD, algorithms in references [19] and [20] is listed in Tab. 2.

Table 2 Recall and AUC values of various models

Model	Number of experiments	Recall	AUC
EMD	1st time	0.828	0.794
	2nd time	0.842	0.787
Reference [19]	1st time	0.864	0.802
	2nd time	0.929	0.831
Reference [20]	1st time	0.904	0.862
	2nd time	0.932	0.753
Designed algorithm	1st time	0.933	0.969
	2nd time	0.956	0.978

In Tab. 2, in the first experiment, the recall rate of the CEEMD-SE-WT algorithm was 0.933, which was 12.7%, 7.9%, and 3.2% higher than the traditional EMD's 0.828, reference [19]'s 0.864, and reference [20]'s 0.904. The AUC value of the CEEMD-SE-WT algorithm was 0.969, while the AUC values of traditional EMD, reference [19], and reference [20] were 0.794, 0.802, and 0.862, representing improvements of 19.5%, 18.3%, and 12.4%. In the second experiment, the recall rate of CEEMD-SE-WT algorithm was 0.956, and the AUC value was 0.978, which was significantly higher than other algorithms. The above results further demonstrated the high accuracy and stability of the CEEMD-SE-WT algorithm in IEVS processing. Finally, to verify the robustness of the proposed CEEMD-SE-WT algorithm, the precision of different algorithms was calculated at Signal-to-Noise Ratio (SNR) of 0 dB, 5 dB, and 10 dB, respectively. The results are shown in Tab. 3.

Table 3 Precision of different algorithms at different SNRs

Index	Precision / %			
Model	EDM	Reference [19]	Reference [20]	CEEMD-SE-WT
SNR = 0 dB	65.32	71.45	75.68	85.67
SNR = 5 dB	72.45	79.32	81.23	89.45
SNR = 10 dB	78.23	84.56	86.34	91.23

From Tab. 3, the precision of the CEEMD-SE-WT algorithm was 85.67% when the SNR was 0dB. The precision of the EMD and methods in reference [19] and reference [20] were 65.32%, 71.45%, and 75.68%, respectively. Compared with the other three methods, the CEEMD-SE-WT algorithm improved the precision by 31.1%, 19.9%, and 13.2%, respectively. When the SNR was 5 dB and 10 dB, the precision of the CEEMD-SE-WT algorithm was 89.45% and 91.23%, respectively, which was significantly higher than other methods. The above results demonstrated that the CEEMD-SE-WT algorithm had stronger resistance to noise interference and higher stability in complex industrial environments.

4.2 Analysis of the Practical Application Effect of Industrial Equipment VSAP Technology Based on EMD-WT

To verify the practical application effect of industrial equipment VSAP technology based on EMD-WT, this study first introduces the coefficient of determination R^2 and calculates the R^2 values of four algorithms to verify the precision of the research algorithms in practical applications, as shown in Fig. 8.

Fig. 8a and Fig. 8b are the R^2 scatter plots of reference [20] and the CEEMD-SE-WT algorithm. The R^2 of the algorithm in reference [20] is 0.954 and the R^2 of CEEMD-SE-WT is 0.987. The R^2 of the CEEMD-SE-WT algorithm is significantly higher than that in reference [20], indicating that CEEMD-SE-WT can more precisely reflect the true features of the signal when processing IEVS, and has higher fitting precision and prediction ability. To further verify its effectiveness in practical applications, the CEEMD-SE-WT algorithm runs 5 times, the processing time is calculated, and the results are compared with EMD, the method in reference [21], and the method in reference [22]. The results are shown in Tab. 4.

Table 4 Average runtime of different algorithms / s

Number of runs	Algorithm			
	EMD	Reference [21]	Reference [22]	CEEMD-SE-WT
1	31.24	29.52	24.63	24.98
2	30.68	30.18	25.88	23.97
3	24.54	28.13	24.74	23.92
4	27.48	26.67	26.52	24.84
5	30.85	27.81	24.23	24.22
Average runtime / s	28.96	28.46	25.20	24.39

In Tab. 4, among the five independent runs, CEEMD-SE-WT has the lowest processing time. Meanwhile, the average processing time of EMD algorithm is 28.96 s, reference [21] is 28.46 s, reference [22] is 25.20 s, and CEEMD-SE-WT is 24.39 s. The average runtime of CEEMD-SE-WT has significantly decreased compared to other algorithms, indicating its high operating efficiency. Finally, the error of CEEMD-SE-WT during training is calculated and compared with traditional EMD. The compares the training and expected values, as exhibited in Fig. 9.

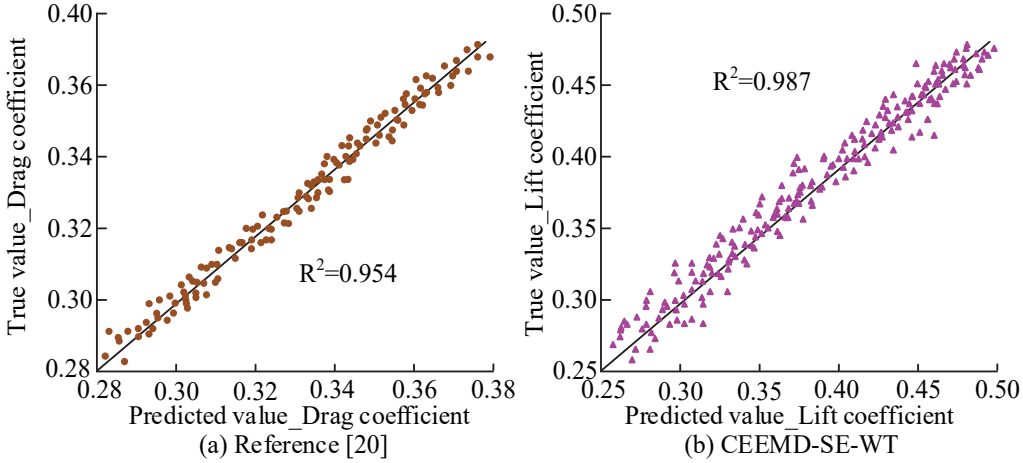

(a) Reference [20] (b) CEEMD-SE-WT

Figure 8 R^2 values of two algorithms

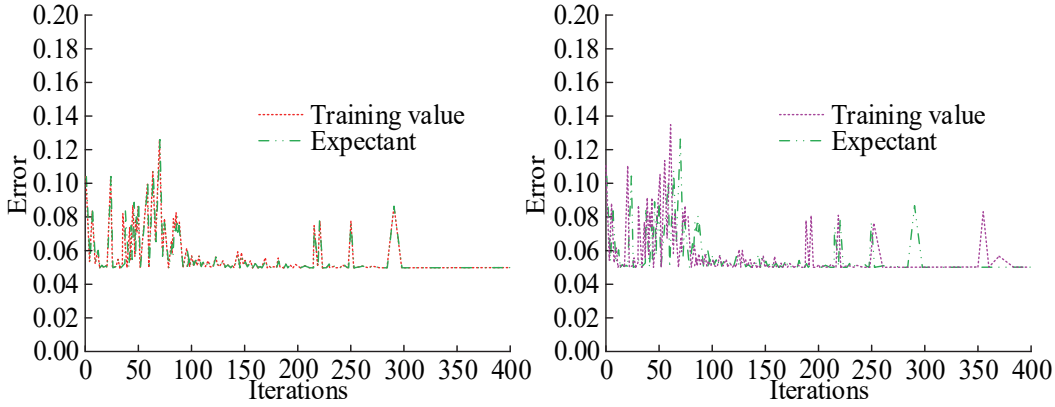

(a) CEEMD-SE-WT (b) EMD

Figure 9 Training errors of different algorithms

In Fig. 9a, the expected training error of the algorithm is between 0.05 and 0.13. The training error of CEEMD-SE-WT basically coincides with the expected error. In Fig. 9b, there is a certain deviation between the training error and the expected value of traditional EMD. This proves that the CEEMD-SE-WT algorithm can better collect and process vibration signals of industrial equipment, and it has high robustness and adaptability.

5 CONCLUSION

In the modern industrial field, monitoring and analyzing equipment vibration signals is crucial as it directly relates to the operational status and fault diagnosis of the equipment. Traditional VSAP technology has issues with precision and efficiency. This study first used CEEMD-SE to decompose the vibration signal, and processed the collected signal through discrete WT, proposing a CEEMD-SE-WT model. The precision of this algorithm in a stable state was 0.93, which was significantly lower than the accuracy of traditional EMD and methods in reference [20], indicating that the designed algorithm has higher precision. The average precision of CEEMD-SE-WT in two experiments reached 92.84% and 90.11%, significantly higher than other methods. Its rejection rate and FAR were also lower, and the computation time was shorter, which proved that CEEMD-SE-WT improved recognition precision while reducing the possibility of false positives, and had higher computational efficiency. Although the EMD-WT method performed well in experiments and could be well applied in fields such as intelligent manufacturing and rail transit, there are still some shortcomings. Although the current algorithm can cope with load changes to a certain extent, its performance may be affected when dealing with more complex IEVs. Meanwhile, in practical industrial scenarios, due to the diverse types of equipment and complex operating conditions, more testing is required to ensure their stability and reliability. Future research will introduce other advanced signal processing techniques combined with the CEEMD-SE-WT algorithm to further enhance its performance. At the same time, collecting vibration data of different types of equipment under various working conditions can enrich the training dataset of the algorithm

and improve its applicability and robustness in practical scenarios.

6 REFERENCES

[1] Patange, A. D., Pardeshi, S. S., Jegadeeshwaran, R., Zarkar, A., & Verma, K. (2023). Augmentation of decision tree model through hyper-parameters tuning for monitoring of cutting tool faults based on vibration signatures. *Journal of Vibration Engineering & Technologies*, *11*(8), 3759-3777. https://doi.org/10.1007/s42417-022-00781-9

[2] Khalil, A. F. & Rostam, S. (2024). Machine learning-based predictive maintenance for fault detection in rotating machinery: A case study. *Engineering, Technology & Applied Science Research*, *14*(2), 13181-13189. https://doi.org/10.48084/etasr.6813

[3] Luque, A., Campos, O. D., Mazzoleni, M., Ferramosca, A., Previdi, F., Carrasco, A. (2025). Use of artificial intelligence techniques in characterization of vibration signals for application in agri-food engineering. *Applied Intelligence*, 55(6), 1-24. https://doi.org/10.1007/s10489-025-06424-2

[4] Jauhari, K., Rahman, A. Z., Al, H. M., Widodo, A., & Prahasto, T. (2024). Building digital-twin virtual machining for milling chatter detection based on VMD, synchro-squeeze wavelet, and pre-trained network CNNs with vibration signals. *Journal of Intelligent Manufacturing*, *35*(7), 3083-3114. https://doi.org/10.1007/s10845-023-02195-0

[5] Zhang, S., Zhou, J., Wang, E., Zhang, H., Gu, M., & Pirttikangas, S. (2022). State of the art on vibration signal processing towards data-driven gear fault diagnosis. *IET Collaborative Intelligent Manufacturing*, *4*(4), 249-266. https://doi.org/10.1049/cim2.12064

[6] Iqbal, M. & Madan, A. K. (2022). CNC machine-bearing fault detection based on convolutional neural network using vibration and acoustic signal. *Journal of Vibration Engineering & Technologies*, *10*(5), 1613-1621. https://doi.org/10.1007/s42417-022-00468-1

[7] Chu, W. L., Xie, M. J., Chang, Q. W., & Yau, H. T. (2022). Research on the recognition of machining conditions based on sound and vibration signals of a CNC milling machine. *IEEE Sensors Journal*, *22*(7), 6364-6377. https://doi.org/10.1109/JSEN.2022.3150751

[8] Svinth, C. N., Wallace, S., Stephenson, D. B. et al. (2022). Identifying abnormal CFRP holes using both unsupervised and supervised learning techniques on in-process force, current, and vibration signals. *International Journal of Precision Engineering and Manufacturing*, *23*(6), 609-625. https://doi.org/10.1007/s12541-022-00641-2

[9] Hosseinpour, Z. M, Omid, M., & Biabani, A. E. (2022). Fault diagnosis of tractor auxiliary gearbox using vibration analysis and random forest classifier. *Information Processing in Agriculture*, *9*(1), 60-67. https://doi.org/10.1016/j.inpa.2021.01.002

[10] Mohammed, N. A., Abdulateef, O. F., & Hamad, A. H. (2023). An IoT and machine learning-based predictive maintenance system for electrical motors. *Journal Européen des Systèmes Automatisés*, *56*(4), 651-656. https://doi.org/10.18280/jesa.560414

[11] Aljemely, A. H., Xuan, J., Al, A. O., & Jawad, F. K. (2022). Intelligent fault diagnosis of rolling bearings based on LSTM with large margin nearest neighbor algorithm. *Neural Computing and Applications*, *34*(22), 19401-19421. https://doi.org/10.1007/s00521-022-07353-8

[12] Chen, X., Hu, X., Wen, T., & Cao, Y. (2023). Vibration signal-based fault diagnosis of railway point machines via double-scale CNN. *Chinese Journal of Electronics*, *32*(5), 972-981. https://doi.org/10.23919/cje.2022.00.229

[13] Cai, L., Hu, D., Zhang, C., Yu, S., & Xie, J. (2022). Tool vibration feature extraction method based on SSA-VMD and SVM. *Arabian Journal for Science and Engineering*, *47*(12), 15429-15439. https://doi.org/10.1007/s13369-022-06635-6

[14] Gu, J., Peng, Y., Lu, H., Chang, X., Cao, S., Chen, G., & Cao, B. (2022). An optimized variational mode decomposition method and its application in vibration signal analysis of bearings. *Structural Health Monitoring*, *21*(5), 2386-2407. https://doi.org/10.1177/14759217211057444

[15] Al-Haddad, L. A., Jaber, A. A., Hamzah, M. N., & Fayad, M. A. (2024). Vibration-current data fusion and gradient boosting classifier for enhanced stator fault diagnosis in three-phase permanent magnet synchronous motors. *Electrical Engineering*, *106*(3), 3253-3268. https://doi.org/10.1007/s00202-023-02148-z

[16] Jaros, R., Byrtus, R., Dohnal, J., Dohnal, J., Danys, L., Baros, J., Koziorek, J., Zmij, P., & Martinek, R. (2023). Advanced signal processing methods for condition monitoring. *Archives of Computational Methods in Engineering*, *30*(3), 1553-1577. https://doi.org/10.1007/s11831-022-09834-4

[17] Zhao, W., Lv, Y., Liu, J., Lee, C. K., & Tu, L. (2023). Early fault diagnosis based on reinforcement learning optimized-SVM model with vibration-monitored signals. *Quality Engineering*, *35*(4), 696-711. https://doi.org/10.1080/08982112.2023.2193255

[18] Mou, W. P., Zhu, S. W., Jiang, Z. X., & Song, G. (2022). Vibration signal-based chatter identification for milling of thin-walled structure. *Chinese Journal of Aeronautics*, *35*(1), 204-214. https://doi.org/10.1016/j.cja.2020.09.029

[19] Chao, Q., Gao, H. H., Tao, J. F., Wang, Y., Zhou, J., & Liu, C. (2022). Adaptive decision-level fusion strategy for the fault diagnosis of axial piston pumps using multiple channels of vibration signals. *Science China Technological Sciences*, *65*(2), 470-480. https://doi.org/10.1007/s11431-021-1904-7

[20] Hammood, A. S., Taki, A. G., Ibrahim, N. S., Mohammed, J. G., Jasim, R. K., & Jasim, O. M. (2024). Optimizing Failure Diagnosis in Helical Gear Transmissions with Stochastic Gradient Descent Logistic Regression using Vibration Signal Analysis for Timely Detection. *Journal of Failure Analysis and Prevention*, *24*(1), 71-82. https://doi.org/10.1007/s11668-023-01814-5

[21] Alberts, M., St. John, S., Jared, B., Karandikar, J., Khojandi, A., Schmitz, T., & Coble, J. (2024). Chatter detection in simulated machining data: a simple refined approach to vibration data. *The International Journal of Advanced Manufacturing Technology*, *132*(9), 4541-4557. https://doi.org/10.1007/s00170-024-13590-z

[22] Joung, B. G., Nath, C., Li, Z., & Sutherland, J. W. (2024). Bearing anomaly detection in an air compressor using an LSTM and RNN-based machine learning model. *The International Journal of Advanced Manufacturing Technology*, *134*(7), 3519-3530. https://doi.org/10.1007/s00170-024-14322-z

Contact information:

Guofu WEI
(Corresponding author)
Western Pipeline Company,
Pipe China, Urumqi, 830010, XinJiang, China
E-mail: wgf18609463161@163.com

Guanlin WANG
Western Pipeline Company
Pipe China, Urumqi, 830010, XinJiang, China
E-mail: xbgdwangguanlin@163.com